JOURNAL OF NANO- AND ELECTRONIC PHYSICS
Vol. **8** No 1, 01040(5pp) (2016)

ЖУРНАЛ НАНО- ТА ЕЛЕКТРОННОЇ ФІЗИКИ
Том **8** № 1, 01040(5cc) (2016)

An Experimental Insight into the ZnO Thin Films Properties Prepared by Dip Coating Technique

M. Benhaliliba[1], Y.S. Ocak[2]

[1] *Material Technology Department, Physics Faculty, USTOMB University, BP1505 Oran, Algeria*
[2] *Dicle University, Education Faculty, Science Department, 21280 Diyarbakir, Turkey*

(Received 04 August 2015; revised manuscript received 02 March 2016; published online15 March 2016)

The physical properties of the pure and metal doped ZnO films are investigated using a low cost dip coating technique. The films have grown slowly onto a glass substrate at room temperature. Based on X-ray pattern parameters are extracted such as grain size, lattice parameters. Optical measurements within the UV-Vis band give us the transmittance of films (> 80 %) and optical band gap. Using the Hall Effect measurement (HMS) in room temperature, we determine the bulk density of charge carriers, mobility and their electrical resistivity.

Keywords: Zinc oxide, Film synthesis, Metal doping, Dip coating, Structural parameters, Transmittance, Optical band gap, Resistivity.

DOI: 10.21272/jnep.8(1).01040

PACS numbers: 77.84.Bw, 68.47.Gh

1. INTRODUCTION

ZnO is the multifunctional material which attracted many researchers during the last decades. As film, it is produced by many processes like spray pyrolysis, sputtering, spin and dip coating [1-4]. We find zinc oxide in many applications such as ultraviolet light emitters and thin film transistors [5-6]. In order to study the influence of molarity on the ZnO layer properties, the films are prepared by low cost dip coating process. We select the zinc molarity within the 0.2-0.5 mol/litre range. Furthermore, at kept zinc acetate molarity of 0.4 mol/litre, the effect of metal doping at various rates on ZnO film properties is investigated.

2. PREPARATION OF LAYERS

For the dip-coating route, the substrate is pulled vertically from the coating bath at a constant speed V as sketched in Fig. 1. The entrained liquid by the moving substrate splits into two at the free surface (point *S*) in a viscous boundary layer, returning the outer layer to the bath. When the mounting moving flux is balanced above the stagnation point S due to evaporation of the solvents, a continuing and position-stable film is formed with respect to the coating bath surface. Inside the drying process, the colloids are gradually concentrated by evaporation, leading to aggregation, gelation, and final drying to synthesize a type of a dry gel or xerogel film. If the substrates' speed (V) and liquid viscosity (η) are lower, e.g. in the case of the sol–gel coating, the thickness (it) of the wet film is then expressed as [7]:

$$t = \left(\frac{0.94(\eta V)^{0.67}}{\gamma_s^{0.17}(\rho g)^{0.5}} \right), \qquad (1)$$

where γ_s is the liquid-vapour surface tension, ρ is the liquid density and g is the acceleration of gravity. For a fixed volume of 20 ml of ethanol and different zinc acetate masses mentioned between brackets, the following molarities are obtained 0.2 (0.87 g), 0.3 (1.32 g), 0.4 (1.76 g) and 0.5 (2.19 g). After a stirring at 80 °C, the prepared solutions are clear and homogenous and seem to oil which reveals a viscous bath. As soon as the bath is ready, the glass substrates are slowly dipped into the solution during 1 min and then removed and dried at 120 °C on the hotplate. The process of dip is repeated 10 times and an annealing procedure of samples is then achieved at 400 °C for 5 hours. For doping the $SnCl_2$, $2H_2O$, Fe_2Cl_3, 6 H_2O, Al_3NO_3, $9H_2O$ and anhydrous Cu acetate precursors are used.

3. RESULTS AND DISCUSSIONS

The samples prepared by dip coating process are classified in three sets. The first one is composed of pure zinc oxide layers at different zinc amounts (0.2-0.5 mol/l) while the second set is formed by 2-20 % Sn doped ZnO layers. 2-3 % Fe, 12 % Al and 10 % Cu doped ZnO form the third set.

3.1 Structural Parameters

Figure 2 shows the XRD peaks of the dip coated ZnO at several zinc amounts in the starting solution Fig. 2I, Sn, Al and Cu-doped ZnO layers Fig. 2II, Fig. 2III respectively. As gathered in Table 1, the main orientations exhibited by ZnO layers (1st set) are (002) and (101) which are located within 34.4°-34.5° and 34.5°-35.7° angle ranges respectively, according to JCPDS: 36-1451 card, (002) plane is peaked at 34.42°. The d-space (Å) varies from 2.47 to 2.60 nm. A slight angle shift is recorded from 0.4 10^{-3} to 0.1 rad as a result of Zn amount. Based on structural data extracted from X-ray pattern the grain size (nm) is assessed within the 14.9-23.8 range according to the (002) direction. Using X-ray pattern, the average lattice parameters a and c are determined and found to be 3.2 and 5.18 Å. Doped with tin at several concentration, ZnO layers show a slight shift to higher Bragg angle for (002) orientation (as indicated by arrow in Fig. 2) whereas the (101) is shifted towards high 2θ angle, this displacement of peaks is due to cation insertion in host lattice.

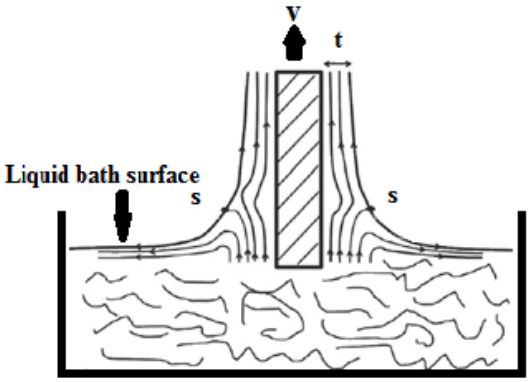

Fig. 1 – Schematic diagram of the dip coating techniques

A (002)-oriented wurtzite hexagonal structure with a lattice parameters of 3.3 Å and 5.2 Å was confirmed by X-ray diffraction. The As-grown layers produced by dip coating route onto glass exhibit a (002) preferential orientation as indicated by arrow in Fig. 2 (I, II and III). The intensity of the (002) peak is improved by high molarity and doping level in particular Al cation. Based on Scherrer formula prior cited [8] the grain size is determined.

The grain size according to (002) orientation varies within 14-28 nm as a result of Zn amount in the solution as tabulated below (Table 1). When ZnO films are doped, it increases till 59 nm as listed in Tables 1 and 2. Furthermore, the X-ray pattern reveals a plane shift

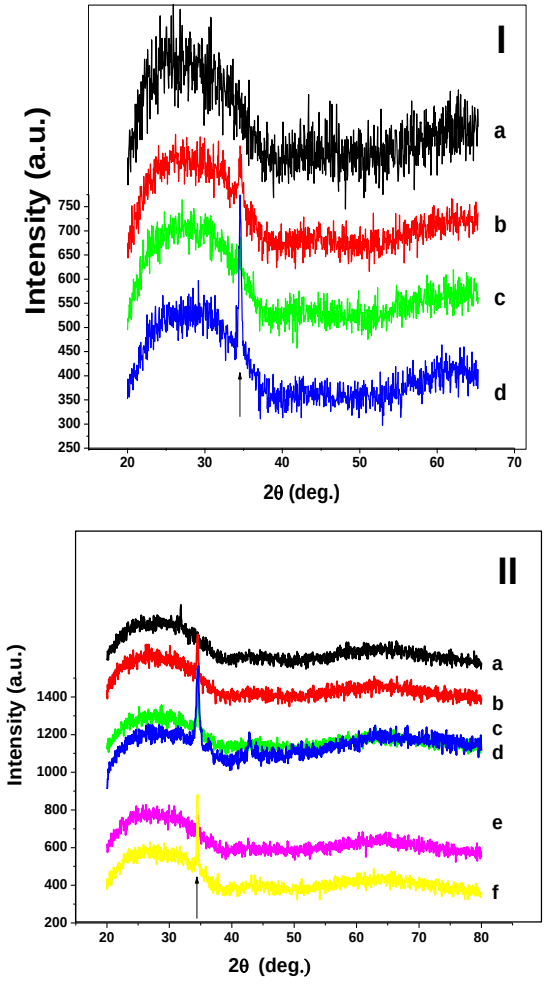

towards the high 2θ Bragg angle as listed in Tables 1-3. A strong orientation of c-axis (002) perpendicular to the substrate is reported by Lee for indium ZnO thin films [9]. The films show a polycrystalline structure with important (002) direction. Indeed, this reflection peaked at around 34.45°, identifies the wurtzite structure of our as-grown ZnO and MZO layers. An increase in Zn amount and a metallic cation doping change the peak location from 34.4° to 36.27° and 36.67° respectively as listed in Tables 1-3. The lattice parameters a and c are also influenced by the Zn amount and metallic (Sn, Al and Cu) cation doping and found to be changed around the values of 3.21 Å and 5.18 Å as seen in Tables 2 and 3. It is found in literature that a and c are of 3.24 Å and 5.20 Å for both pure and doped ZnO [10].

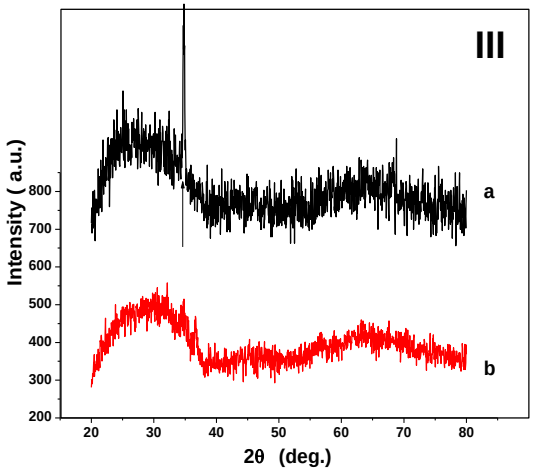

Fig. 2 – XRD spectra for different molarities (I), 2 (a), 3 (b), 5 (c), 10 (d), 15 (e) and 20 (f) % Sn-doped (II), Al (a) and copper (b) -doped(III) ZnO films in the 20°-80° (2θ) range

3.2 Optical Characterization

The transmittance versus photon wavelength is displayed in the Fig. 3. At the middle of visible range of 550 nm, the obtained values of transmittance are found within 88-91 % range for pure layers and 75-90 % range for Sn doped ZnO layers. The transmittance becomes lower (73-80 %) for the Al and Cu doped ZnO films. Both, Al and Fe doping increase the transmittance till 88 % and 83 % for ZnO films as reported previously [11, 3]. Sn and Al ions decrease a little the optical property in visible range of the as-synthesized ZnO films as mentioned in prior work [12]. The transmittance still roughly constant around a higher value in IR band, similar trends is reported by Lehraki et al. [13]. The optical gap is determined by the variation of the $(\alpha h\nu)^2$ versus photon energy $h\nu$ (not shown here). This gap goes from 4.35 to 4.42 eV for the pure ZnO films. Whereas, it varies within the 4.40-4.45 eV energy range for the doped ones. It is mentioned that 3.27 and 3.26 eV are the obtained values of optical band gaps for the pure and Al-doped ZnO [14]. The highest transmittance at a wavelength of 550 nm is obtained for the ZnO layers, which have grown at 400 °C (> 84 %) as reported in recent work [15].

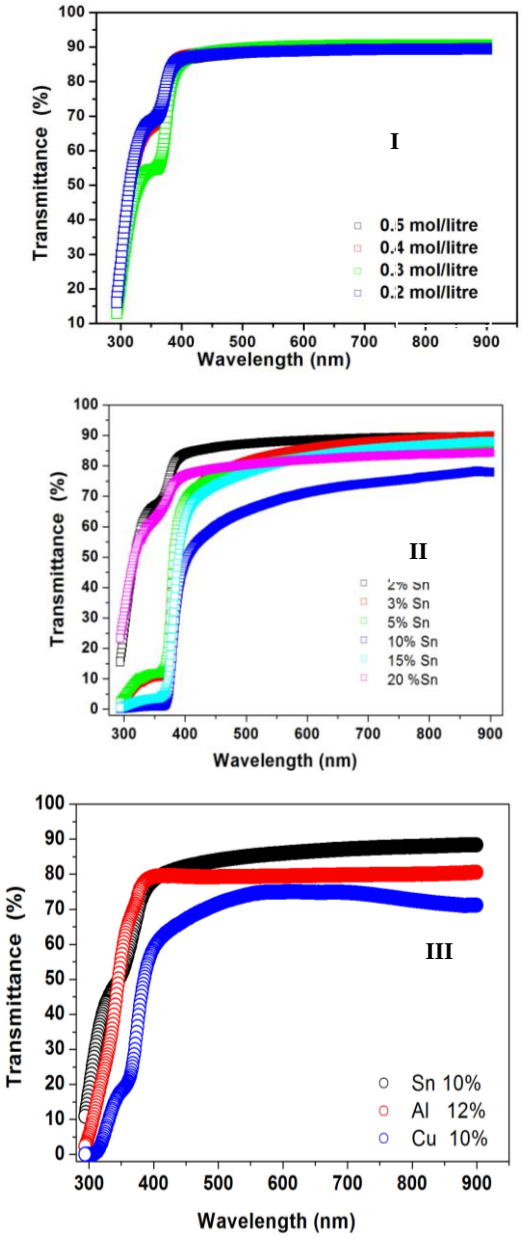

Fig. 3 – Transmittance vs. photon wavelength of undoped at several Zn proportions (I), Sn- (II), Al, Cu (III)-doped ZnO produced by dip coating route

It is revealed that our pure ZnO layers exhibit a high transparency $T > 85$ %) within the visible range and transmittance reaches a high point of 95 % for the lowest molarity of 0.2 mol/liter as shown in Fig. 3.I. Therefore, the transmittance diminishes as molarity increases due to high deposited quantity of ZnO at high molarity. Over 60 %, the transmittance profile indicates a rough square edge in particular for the concentration of 0.2 mol/l as sketched in Fig. 3. The 5, 10, 15 and 20 % tin doped ZnO films are less transparent compared to pure ones. The square edge becomes slight as a result of Sn concentration as shown in Fig.3.II.

3.3 HMS Measured Values

At room temperature, the electrical parameters of the samples are measured via Hall effect measurement (HMS), using a magnetic field of 0.58 T, as shown in Fig. 4 and 5, and are given in Tables 4-5.

A bulk density of holes (p type) varying from 3.7×10^{12} to 13.4×10^{12} cm^{-3} is confirmed by samples of pure as-grown ZnO layers when molarity increases from

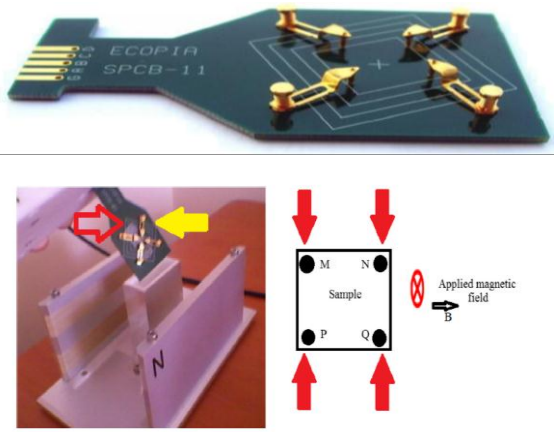

Fig. 4 – Hall measurement apparatus of pure and M (Sn, Al, Cu)-doped ZnO grown onto glass substrate; the films are kept by four Au probes (red arrow) as signed by yellow arrow (left). As shown at right, the scheme of the samples, the four contacts M, N, P, Q, and the magnetic field is applied perpendicularly to the sample [4, 16]

Table 1 – The structural parameters of pure ZnO films at several molarities

Pure ZnO films concentration (mol/l)	(hkl) orientation	2θ (Deg.)	d_{hkl} (Å)	$\Delta(2\theta)$ (10^{-3} rad)	Grains size D (nm)	Peak Intensity (arb. u.)	Lattice parameters (Å)		
							c	a	c/a
0.2	(002)	34.41	2.60	10.14	14.95	54.0	5.21	3.31	1.5
0.2	(101)	35.72	2.52	0.43		54.0			
0.3	(002)	34.54	2.59	6.97	21.76	56.10	5.19	3.29	1.5
0.3	(101)	35.96	2.49	96.90		44.6			
0.4	(002)	34.53	2.59	6.37	23.80	52.9	5.19	3.25	1.6
0.4	(101)	36.27	2.47	0.44		45.8			
0.5	(002)	34.54	2.5943	5.350	28.34	77.4	5.19	3.25	1.6
0.5	(101)	36.31	2.4720	33.99		42.4			

Table 2 – The structural parameters of Sn doped ZnO films at several doping levels

Sn doped ZnO films concentration (mol/l)	(*hkl*) orientation	2θ (Deg.)	d_{hkl} (Å)	$\Delta(2\theta)$ (10^{-3} rad)	Grains size D (nm)	Peak Intensity (arb.u.)	Lattice parameters (Å)		
							c	*a*	*c*/*a*
Sn 2 %	(002)	34.54	2.59	6.96	21.78	88.0	5.19	3.25	1.6
	(101)	36.27	2.47	0.45		43.4			
Sn 3 %	(002)	34.54	2.59	4.35	35.12	117.2	5.19	3.24	1.6
	(101)	36.36	2.47	6.91		89.8			
Sn 5 %	(002)	34.49	2.59	4.10	37.00	82.26	5.19	3.30	1.5
	(101)	35.79	2.51	0.97		50.0			
Sn 10 %	(002)	34.57	2.59	2.56	59.16	55.20	5.18	3.26	1.6
	(101)	36.21	2.48	3.91		42.40			
Sn 15 %	(002)	34.49	2.60	3.59	42.28	70.4	5.19	3.25	1.6
	(101)	36.28	2.47	0.47		46.0			
Sn 20%	(002)	34.58	2.59	3.42	44.38	72.5	5.18	3.26	1.6
	(101)	36.19	2.48	2.92		38.5			

Table 3 – The structural parameters of M-doped ZnO films at several metal amounts

M-doped ZnO Films (M: Al, Cu) concentration (mol/l)	(*hkl*) orien-tation	2θ (Deg.)	d_{hkl} (Å)	$\Delta(2\theta)$ (10^{-3} rad)	Grains size *D* (nm)	Peak Inten-sity (arb.u.)	Lattice parameters (Å)		
							c	*a*	*c*/*a*
Al 12 %	(002)	34.43	2.57	4.64	32.70	91.00	5.15	3.43	1.5
	(101)	35.78	2.51	0.42		45.60			
Cu 10 %	(002)	34.69	2.58	17.07	8.89	49.40	5.17	3.21	1.6
	(101)	36.67	2.45	12.73		46.90			

Table 4 – Electrical parameters of pure dip coated ZnO films determined by HMS measurement

Pure ZnO mol/l	type	Bulk density ($\times10^{12}$) cm^{-3}	Mobility (cm²/Vs)	Resistivity ($\times10^4$ Ω.cm)	Hall constant R_H ($\times10^4$ Ω.cm)
0.2	*p*	7.36	15.65	5.42	84.76
0.3	*p*	5.91	19.23	5.49	105.7
0.4	*p*	3.76	29.49	5.63	166.1
0.5	*p*	13.41	8.689	5.36	46.55

Table 5 – Electrical parameters of Sn-doped ZnO films determined by HMS measurement

Sn doped ZnO (%)	type	Bulk density ($\times10^{12}$) cm^{-3}	Mobility (cm²/Vs)	Resistivity ($\times10^4$ Ω.cm)	Hall constant R_H ($\times10^4$ Ω.cm)
2	*p*	1.70	57.52	6.36	365.8
3	*n*	– 3.73	0.90	175.1	– 167.4
5	*p*	10.73	10.63	5.48	58.19
10	*p*	29.67	3.93	5.36	21.04
15	*p*	7.05	16.72	5.29	88.56
20	*p*	10.81	10.85	5.32	57.74

Table 6 – Electrical parameters of m(Al, Cu)-doped ZnO films determined by HMS measurement

M doped ZnO (%)	type	Bulk density ($\times10^{12}$) cm^{-3}	Mobility (cm²/Vs)	Resistivity ($\times10^4$ Ω.cm)	Hall constant R_H ($\times10^4$ Ω.cm)
Al 12 %	*p*	2.59	26.2	9.16	240.6
Cu 10 %	*p*	19.32	5.73	5.63	32.3

Fig. 5 – Hall measurement apparatus ecopia HMS-3000

0.2 to 0.5 mol/litre while resistivity still constant around 5.4×10^4 Ω.cm as tabulated below (Table 4). The Sn- doped samples exhibit a *p*-type except 3 %. The mobility is higher and equals to 57.5 cm²/Vs for 2 % Sn doping level and reveals a resistivity of 6.3×10^4 Ω.cm as seen in Table 5. Al doping increases the charge mobility while Cu cation decreases it as indicated in Table 6.

4. CONCLUSION

The pure and metallic doped films of ZnO are successfully produced by dip coating process. The films are polycrystalline and crystallize according a wurtzite structure with a (002) preferential orientation. The average grain size is about lower and increases with doping level. The as grown ZnO layers present a high transmittance > 80 % in visible range and a high resistivity > 10^4 Ω.cm at room temperature.

AKNOWLEDGEMENTS

This work is included in CNEPRU project N° D01920120039 supported by High Teaching and Scientific Research Ministry www.mesrs.dz and Oran University of Sciences and Technology www.univ-usto.dz. The authors are grateful for the assistance of DUBTAM center Dicle University Ditarbakir Turkey and The Head and staff of the virtual library of SNDL https://www.sndl.cerist.dz.

REFERENCES

1. C.E. Benouis, M. Benhaliliba, Z. Mouffak, A. Avila-Garcia, A. Tiburcio-Silver, M. Ortega Lopez, R. Romano Trujillo, Y.S. Ocak, *J. Alloy. Compd.* **603**, 213 (2014).
2. Y.S. Ocak, *J. Alloy. Compd.* **513**, 130 (2012).
3. M. Benhaliliba, C.E. Benouis, M.S. Aida, Y.S. Ocak, F. Yakuphanoglu, *Int. J. Nanoparticles* **6** No 2/3, 239 (2013).
4. M. Benhaliliba, Y.S. Ocak, A. Tab, *J. Nano- Electron. Phys.* **5** No 3, 03001 (2013).
5. Hui-Huan Guan, Pei-De Han, Yu-Ping Li, Xue Zhang, Qi-Na Zhang, Li PingWang, Rui-Zhen Zhang, *Optik* **124**, 198 (2013).
6. Sheng Xu, Zhong Lin Wang, *Nano Res.* **4** No 11, 1013 (2011).
7. L.D. Landau, V.G. Levich, *Acta Phys.-Chim. Sin.* **17**, 42 (1942).
8. Mostefa Benhaliliba, *J. New Technol. Mater.* **4** No 1, 11 (2014).
9. C. Lee, K. Lim, J. Song, *Sol. Energy Mater. Sol. C.* **43**, 37 (1996).
10. M. Benhaliliba, C.E. Benouis, M.S. Aida, F. Yakuphanoglu, A. Sanchez Juarez, *J. Sol-Gel Sci. Technol.* **55**, 335 (2010).
11. M. Benhaliliba, C.E. Benouis, M.S. Aida, A. Sanchez Juarez, F. Yakuphanoglu, A. Tiburcio Silver, *J. Alloy. Compd.* **506**, 548 (2010).
12. M. Benhaliliba, C.E. Benouis, A. Tiburcio-Silver, Y.S. Ocak, *EPJ Web of Conferences* **44**, 03003 (2013).
13. N. Lehraki, M.S. Aida, S. Abed, N. Attaf, A. Attaf, M. Poulain, *Curr. Appl. Phys.* **12**, 1283 (2012).
14. Mostefa Benhaliliba, *DUFED Dicle. University Journal Institute of Naturel and Applied Science Journal* **3** No 1, 79 (2014).
15. M. Benhaliliba, A. Tiburcio-Silver, A. Avila-Garcia, A. Tavira, Y.S. Ocak, M.S. Aida, C.E. Benouis, *J. Semiconductors* **36** No 8, 083001 (2015).
16. M. Benhaliliba, C.E. Benouis, Y.S. Ocak, F. Yakuphanoglu, *J. Nano- Electron. Phys.* **4** No 1, 01011 (2012).